Electronic Supplementary Material (ESI) for Energy & Environmental Science. This journal is © The Royal Society of Chemistry 2018

Electronic Supplementary Information

Additive-induced Miscibility Regulation and Hierarchical Morphology Enables 17.5% Binary Organic Solar Cells

*Jie Lv, ‡[a,b] Hua Tang,‡[a,b,c] Jiaming Huang, [c] Cenqi Yan, [c] Kuan Liu, [c] Dingqin Hu, [a] Ranbir Singh, [d] Jawon Lee,[e] Shirong Lu, *[a] Gang Li, *[c] & Zhipeng Kan *[a]*

a. J. Lv, H. Tang, D. Hu, Prof. Z. Kan, Prof. S. Lu, Thin-film Solar Technology Research Center, Chongqing Institute of Green and Intelligent Technology, Chinese Academy of Sciences, Chongqing, 400714, P. R. China. E-mail: lushirong@cigit.ac.cn, kanzhipeng@cigit.ac.cn

b. J. Lv, H. Tang, University of Chinese Academy of Sciences, Beijing 100049, P. R. China

c. H. Tang, Dr. C. Yan, Dr. K. Liu, J. Huang, Prof. G. Li, Department of Electronic and Information Engineering, The Hong Kong Polytechnic University, Hung Hum, Kowloon, Hong Kong SAR, P. R. China. E-mail: gang.w.li@polyu.edu.hk

d. Dr. R. Singh, Department of Energy & Materials Engineering, Dongguk University, Seoul 04620, Republic of Korea

e. Dr. J. Lee, Department of Chemical Engineering and Applied Chemistry, Chungnam National University, Daejeon, 34134, Republic of Korea

Content

1. Device Fabrication

The PM6:Y6 organic solar cells were prepared on glass substrates with tin-doped indium oxide (ITO, 15 Ω/sq) patterned on the surface (device area: 0.1 cm^2). Substrates were prewashed with isopropanol to remove organic residues before immersing in an ultrasonic bath of soap for 15 min. Samples were rinsed in flowing deionized water for 5 min before being sonicated for 15 min each in successive baths of deionized water, acetone and isopropanol. Next, the samples were dried with pressurized nitrogen before being exposed to a UV-ozone plasma for 15 min. PEDOT:PSS was diluted with the same volume of water, a thin layer of PEDOT:PSS (~20 nm) (Clevios AL4083) was spin-coated onto the UV-treated substrates, the PEDOT-coated substrates were subsequently annealed on a hot plate at 160 °C for 15 min, and the substrates were then transferred into the glovebox for active layer deposition.

All solutions were prepared in the glovebox using the donors of PM6 and the acceptor of Y6; The PM6 and Y6 were purchased from organtec.ltd., and the1-fluoronaphthalene(FN), 1-chloronaphthalene(CN) and 1-bromonaphthalene(BN) were purchased from Shanghai Titan Technology Co. , Ltd.. Optimized devices were obtained by dissolving PM6 and Y6 in chloroform (CF) using a D/A ratio of 1:1.2, 1:1.2 with 0.9% FN, 1:1.2 with 0.5% CN and 1:1.2 with 0.6% BN (vol/vol), total concentration of 16 mg/ml. Note: The as-prepared solutions were stirred overnight at room temperature before being spin coat on the PEDOT:PSS substrates. The active layers were spin-coated at an optimized speed of 3000 rpm for time period of 30s, resulting in films of 110 to 120 nm in thickness. The active layers were then thermal annealing (TA) for 10 min at 110 °C.

The next stage is to coat ETL on active layer, about 50 uL PFNBr solution (0.5 mg/ml in Methanol) was spin-coated at 3000 rpm for 20s. Finally, the samples were placed in a thermal evaporator for evaporation of a 90 nm-thick layer of Silver (Ag) evaporated at 2 Å s^{-1}; pressure of less than $2x10^{-6}$ Torr. Following electrode deposition, samples underwent J−V testing.

The current density-voltage (J-V) curves of devices were measured using a Keithley 2400 Source Meter in glove box under AM 1.5G (100 mW cm^{-2}) using a Enlitech solar simulator (purchased from Enli Technology Co., Ltd.). A 2×2 cm^2 monocrystalline silicon reference cell with KG1 filter (purchased from Enli Tech. Co., Ltd., Taiwan). The external quantum efficiency (EQE) was measured by a certified incident photon to electron conversion (IPCE) equipment (QE-R) from Enli Technology Co., Lt. The light intensity at each wavelength was calibrated using a standard monocrystalline Si photovoltaic cell.

2. PV Device Performance Data

Table S1. Summary of PV performance for PM6:Y6-based OSCs with different volume ratio of FN in conventional devices under AM 1.5G 100 mW/cm^2 illumination.

Materials	Condition	V_{OC} [V]	J_{SC} [mA cm^{-2}]	FF [%]	PCE [%]
PM6:Y6 1:1.2	0.5%FN	0.85	25.54	70.7	15.2
	0.6%FN	0.84	26.06	70.6	15.4
	0.7%FN	0.83	26.52	72.6	16.1
	0.8%FN	0.83	26.79	74.4	16.6
	0.9%FN	0.83	26.98	77.8	17.5
	1% FN	0.83	26.03	75.9	16.5

Table S2. Summary of PV performance for PM6:Y6-based OSCs with different volume ratio of BN in conventional devices under AM 1.5G 100 mW/cm^2 illumination.

Materials	Condition	V_{OC} [V]	J_{SC} [mA cm^{-2}]	FF [%]	PCE [%]
PM6:Y6 1:1.2	0.3%BN	0.83	25.13	72.2	15.2
	0.4%BN	0.83	25.84	71.6	15.5
	0.5%BN	0.83	25.96	73.4	15.9
	0.6%BN	0.84	26.00	74.9	16.4
	0.7%BN	0.84	26.08	73.4	16.1
	0.8%BN	0.83	24.90	74.2	15.3

Table S3. Summary of PV performance for PM6:Y6-based OSCs with different additives in conventional devices under AM 1.5G 100 mW/cm^2 illumination. All of cells performed without any treatment.

Materials	Condition	V_{OC} [V]	J_{SC} [mA cm^{-2}]	FF [%]	PCE [%]
PM6:Y6 1:1.2	0.9%FN	0.86	25.70	72.7	16.1
	0.5%CN	0.87	23.89	73.0	15.1
	0.6%BN	0.88	22.56	74.8	14.9

4. Contact angle measurements

Table S4. Summarized Contact Angles of the materials.

Films	Contact Angle (deg)	
	[a] H_2O	[b] formamide,FA
PM6	106.90	82.20
	106.70	82.60
	106.83	81.90
PM6 FN	106.30	85.70
	106.40	85.30
	106.42	85.80
PM6 CN	106.30	84.80
	106.20	84.70
	106.40	84.72
PM6 BN	106.00	86.70
	105.80	86.60
	105.90	86.40
Y6	93.20	71.70
	93.60	71.80
	93.00	72.00
Y6 FN	95.10	76.30
	95.20	76.20
	95.18	76.70
Y6 CN	93.60	71.00
	93.40	70.70
	93.30	70.60
Y6 BN	94.80	78.90
	95.10	78.40
	95.20	78.70

[a] Deionized water; [b] formamide;

Table S5. Summarized Average Contact Angles and Surface FreeEnergy Parameters of the materials

Films	Contact Angle (deg)		surface free energy,γ (mJ m^{-2})
	[a] H_2O	[b] formamide,FA	
PM6	106.81(±0.09)	82.23(±0.37)	25.36
PM6 FN	106.37(±0.20)	85.60(±0.03)	20.64
PM6 CN	106.30(±0.10)	84.74(±0.06)	21.62
PM6 BN	105.90(±0.10)	86.57(±0.13)	19.22
Y6	93.27(±0.33)	71.83(±0.17)	27.58
Y6 FN	95.16(±0.04)	76.40(±0.30)	23.76
Y6 CN	93.43(±0.17)	70.77(±0.23)	28.93
Y6 BN	95.03(±0.17)	78.67(±0.23)	21.57

[a] Deionized water; [b] formamide;

The contact angles of the films were performed on a DSA-100 (KRUSS Germany) contact angle meter. Then the surface free energy was calculated by Owens-Wendt method:[1, 2]

$$\gamma_L \times (1 + \cos\theta) = 2 \times \left(\gamma_L^d \cdot \gamma_{sv}^d\right)^{1/2} + 2 \times \left(\gamma_L^p \cdot \gamma_{sv}^p\right)^{1/2} \quad (1)$$

where γ_L and γ_s are surface free energy of the probe liquid and sample, respectively, θ is the contact angle of the sample.

The average contact angles of two liquids (deionized water and formamide) on the various neat films were measured and the results (Test three times separately) in **Table S4**, and the average contact angles and surface energy parameters are summarized in **Table S5**. Then calculate the Flory-Huggins interaction parameter $\chi_{donor-acceptor}$ for blend to show the binary miscibility from

$$K\left(\gamma_{donor}^{1/2} - \gamma_{acceptor}^{1/2}\right)^2 \quad (2)$$

where γ is the surface energy of the material, K is the proportionality constant. [3, 4]

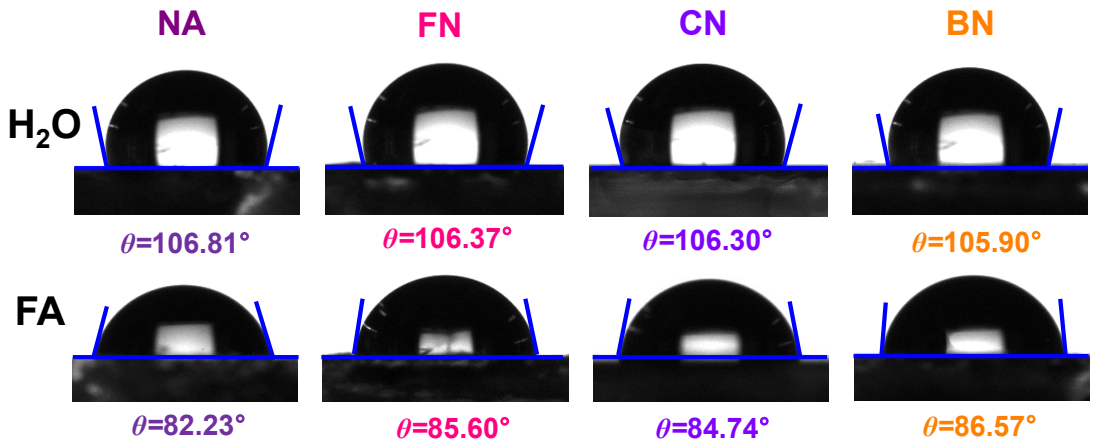

Figure S1. The Deionized water and formamide (FA) contact angles of the pristine PM6 of NA ,FN, CN and BN.

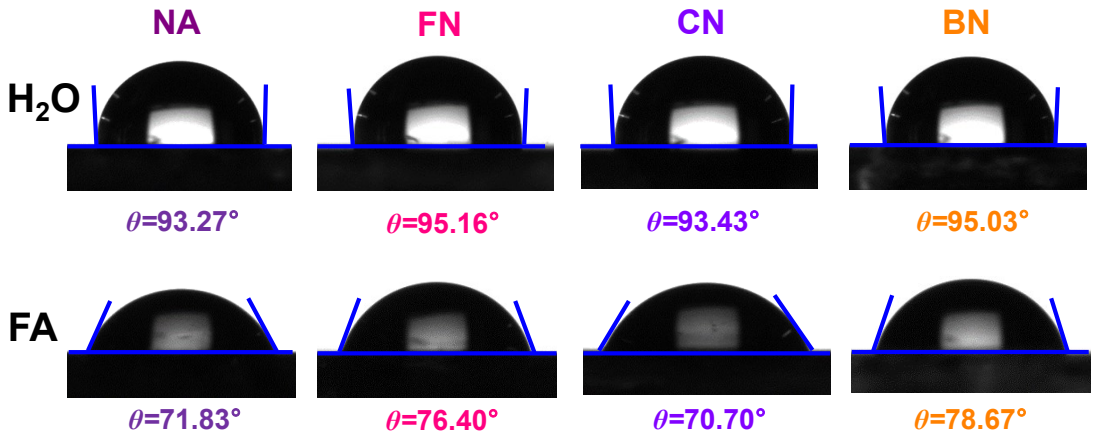

Figure S2. The Deionized water and formamide (FA) contact angles of the pristine Y6 of NA ,FN, CN and BN.

5. Transfer Matrix calculation

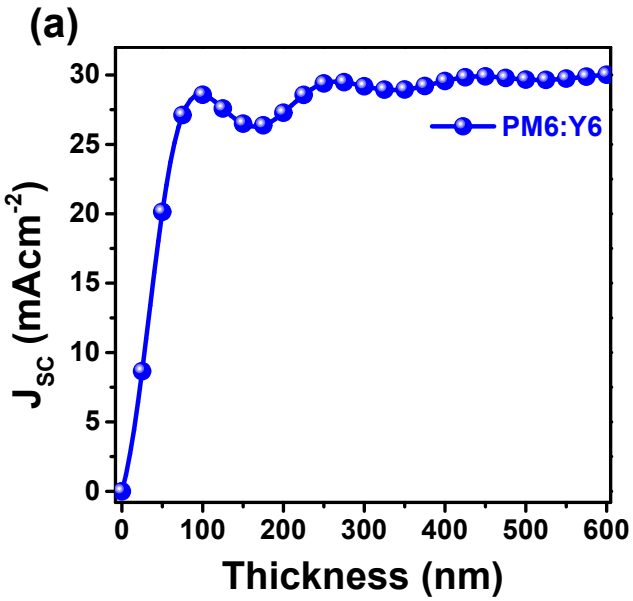

Figure S3. (a) Maximum theoretical J_{SC} plots vs. active layer thickness; curves simulated via transfer matrix for optimized blends of PM6:Y6. The model assumes 100% IQE.

Transfer matrix modeling was used to simulate the maximum theoretical J_{SC} plots as a function of active layer thickness (thickness range: 0-600 nm) for optimized blends of PM6:Y6; the model assumes 100% internal quantum efficiency (IQE). The transfer matrix code for these simulations was developed by George F. Burkhard and Eric T. Hoke; code available from: http://web.stanford.edu/group/ mcgehee/transfermatrix/index.html.[5, 6] The optical constants n and k for the active layers described in Figure S4 and Figure S5.

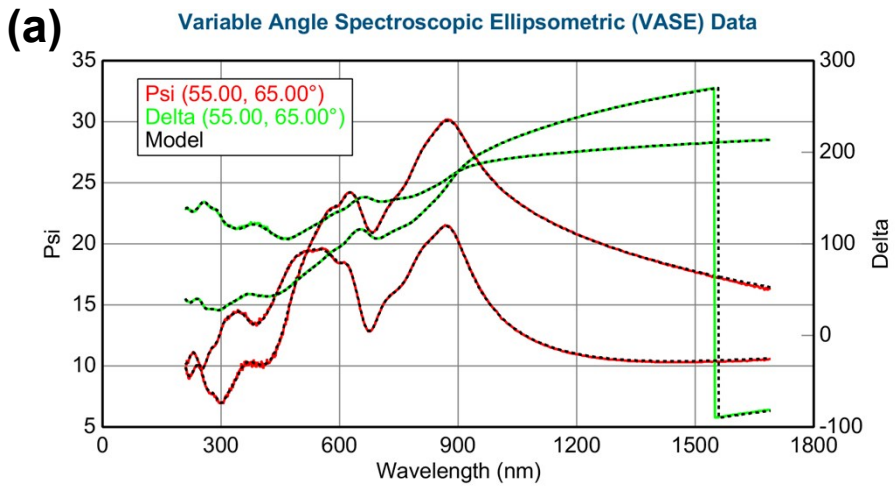

Figure S4. (a) The PM6:Y6 blend film variable angle spectrospotic ellipsornetric (VASE) data and the fittings.

Notes on Ellipsometry (EM) measurements and data analysis:

The films were prepared on optical glasses following the active layer conditions and tested with the M-2000 Ellipsometer. The measured data were fitted with the software CompleteEASE with Gen-Osc models. The fitting quality was evaluated by the MSE values, and MSE values of 2.676 was obtained for the thin film fitting. The thickness value *ca*. 106 nm was obtained from the fitting, in line with the experimental data. The experimental data were well fitted by the models applied as shown in Figure S4.

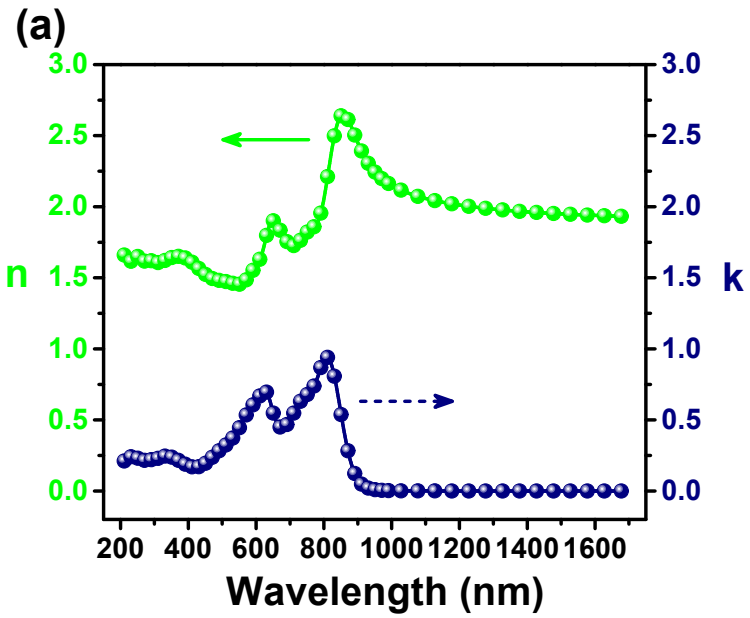

Figure S5. n and **k** values fitted from the ellipsometry measurements.

6. UV-Vis Absorption

UV-vis absorption spectra of PM6:Y6 different additives under thermal annealing were recorded on a PerkinElmer LAMBDA 365 UV-Vis spectrophotometer.

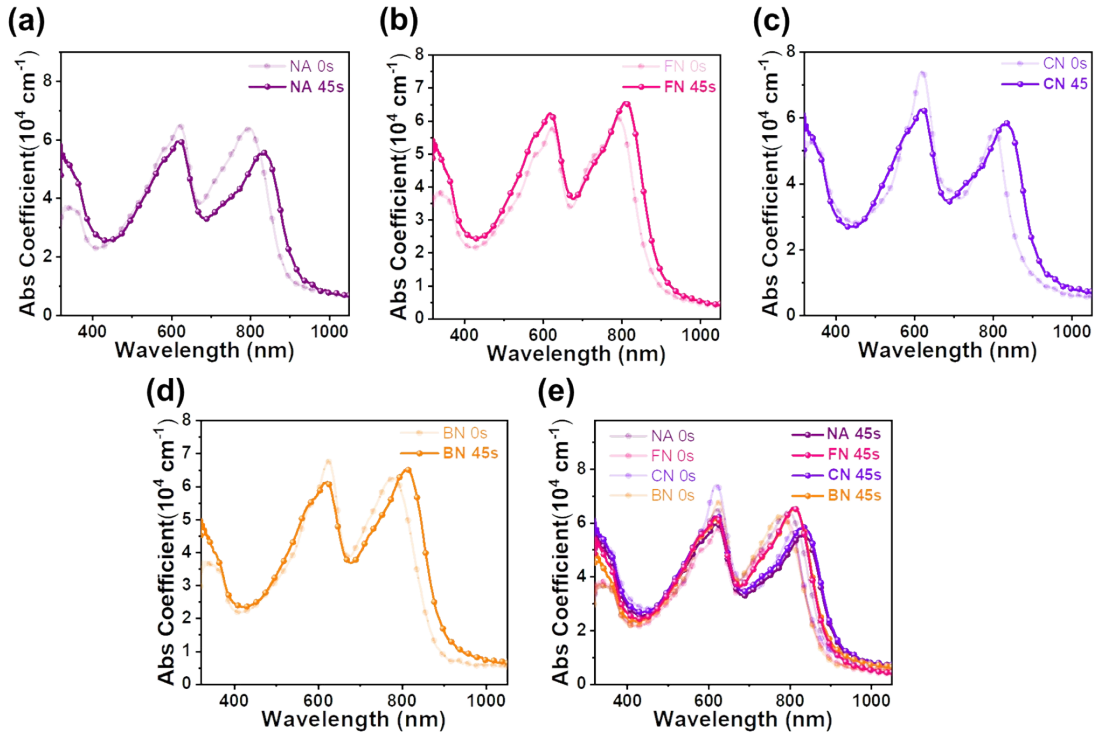

Figure S6. UV-vis absorbance spectra of PM6:Y6 with (a) NA, (b) FN, (c) CN and (d) BN under thermal annealing (TA) of 0 and 45s, (e) UV-vis absorbance spectra of PM6:Y6 (after TA for 0s and 45 s) processed with NA, FN, CN, and BN.

7. Grazing Incidence Wide-angle X-ray Scattering

Grazing-incidence wide-angle X-ray scattering (GIWAXS) was measured at Pohang Light Source (Korea), beam line 3C. Silicon substrates for GIWAXS test were sonicated for 15 min each in successive baths of detergent, DI water, acetone and isopropanol. The substrates were then dried with pressurized nitrogen before being exposed to the UV−ozone plasma for 20 min. The BHJ layers were prepared following methods described in Section of Device Fabrication.

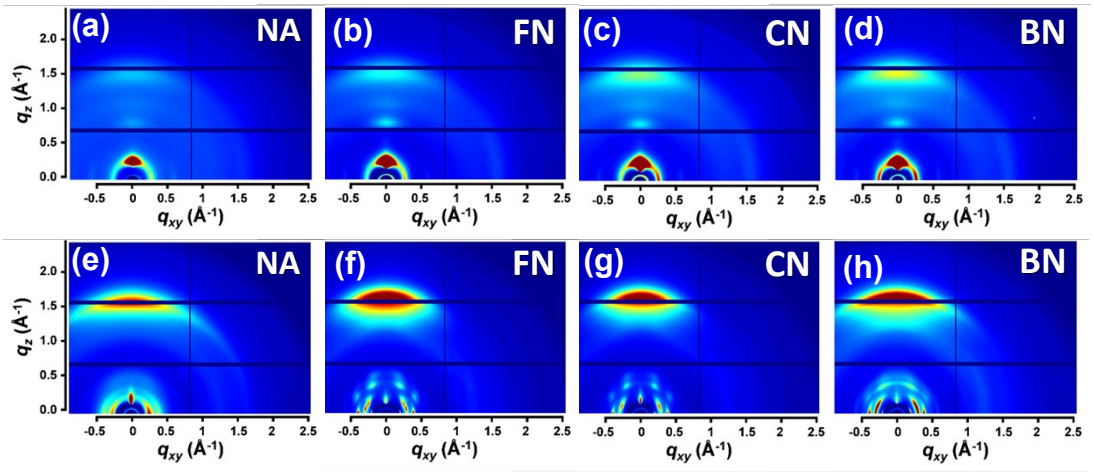

Figure S7. 2D GIWAX patterns of pristine films based on PM6 of (a) NA, (b) FN, (c) CN, (d) BN; 2D GIWAX patterns of pristine films based on Y6 of (e) NA, (f) FN, (g) CN, (h) BN;

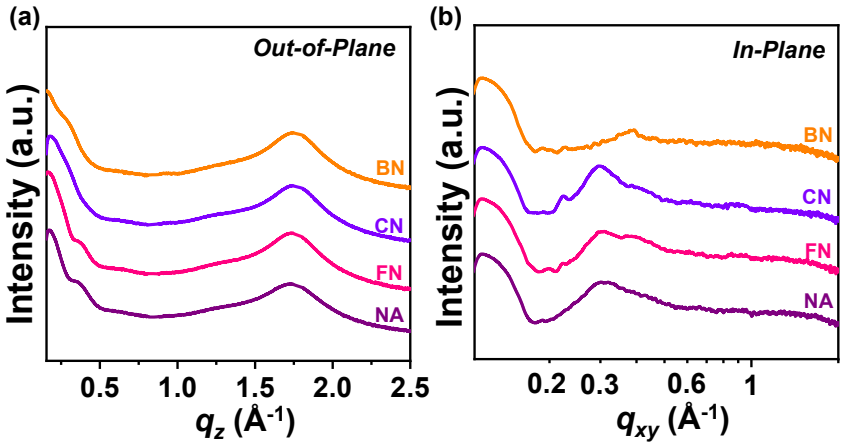

Figure S8. (a) Corresponding GIWAXS intensity profiles along the out-of-plane directions of PM6: Y6 blend films of NA, FN, CN and BN; And (b) corresponding GIWAXS intensity profiles along the in-plane directions of PM6: Y6 blend films of NA, FN, CN and BN.

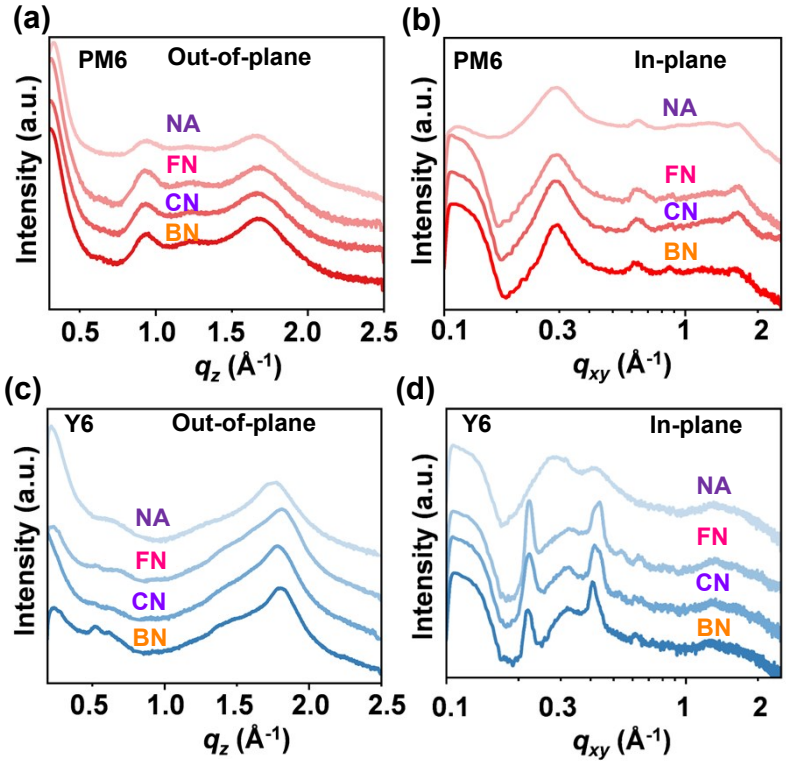

Figure S9. (a) and (c)Corresponding GIWAXS intensity profiles along the out-of-plane directions of PM6 and Y6 pristine films of NA, FN, CN and BN; And (b) and (d) corresponding GIWAXS intensity profiles along the in-plane directions of PM6 and Y6 pristine films of NA, FN, CN and BN.

Table S6. Detailed GIWAXS (100) peak information IP and OOP of NA, FN, CN and BN blend film.

Component	Peak	Peak location (Å^{-1})	FWHM (Å^{-1})	Crystal coherence length(nm)
NA	(100)IP	0.41	0.101	5.60
	(010)OOP	1.7	0.366	1.54
FN	(100)IP	0.32	0.106	5.33
	(010)OOP	1.69	0.332	1.70
CN	(100)IP	0.32	0.071	7.96
	(010)OOP	1.7	0.304	1.86
BN	(100)IP	0.33	0.116	4.87
	(010)OOP	1.69	0.357	1.58

8. Atomic Force Microscopy (AFM) Imaging

Topographic images of the films were obtained from a Bruker atomic force microscopy (AFM) with the type of dimension edge with Scan AsystTM in the tapping mode using an etched silicon cantilever at a nominal load of ~2nN, the scanning rate for a 2 μm×2 μm image size was 0.9 Hz and 5 μm×5 μm image size was 1.0 Hz.

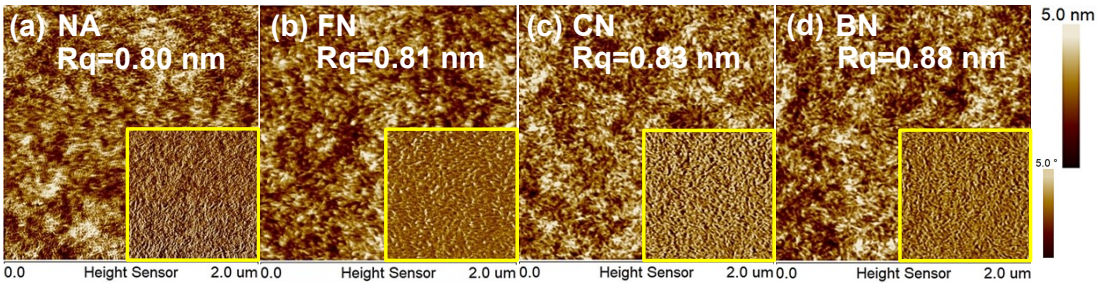

Figure S10. AFM height images with phase images inset of PM6 pristine film of (a) NA, (b) FN, (c) CN, (d) BN**.**

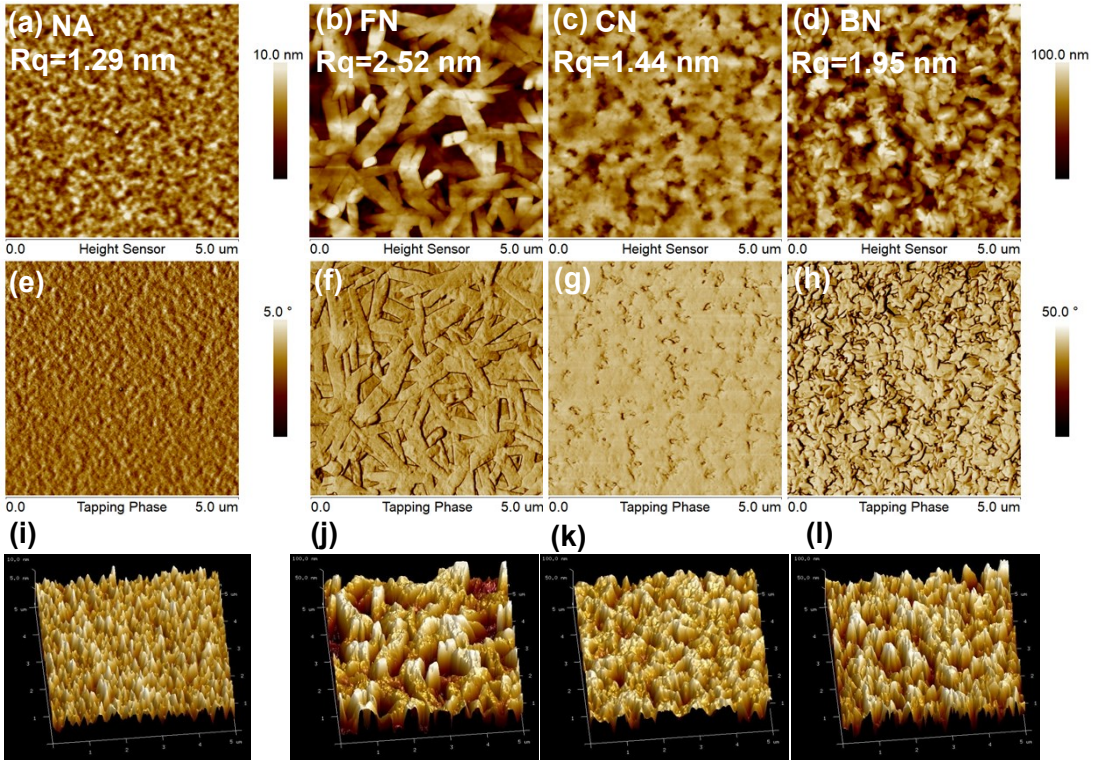

Figure S11. AFM height images of Y6 pristine film of (a) NA, (b) FN, (c) CN, (d) BN, and AFM phase images of Y6 pristine film of (e) NA, (f) FN, (g) CN and (h) BN; Corresponding Three-dimensional (3D) AFM surface roughness images of Y6 pristine film of (i) NA, (j) FN, (k) CN and (l) BN.

9. Transmission Electron Microscopy (TEM) Characterization

Films were spun-cast on PEDOT:PSS-coated glass substrates. The PM6, Y6 and BHJ films were floated off the substrates in deionized water and collected on lacey carbon coated TEM grids (Electron Microscopy Sciences). TEM studies were performed a Thermo Fischer (former FEI) Titan 80-300 TEM equipped with an electron monochromator and a Gatan Imaging Filter (GIF) Quantum 966.

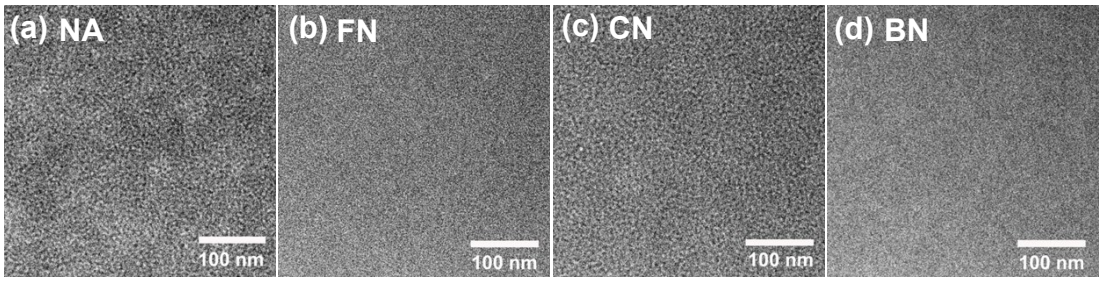

Figure S12. TEM images of PM6:Y6 blend film of (a) NA, (b) FN, (c) CN, (d) BN**.**

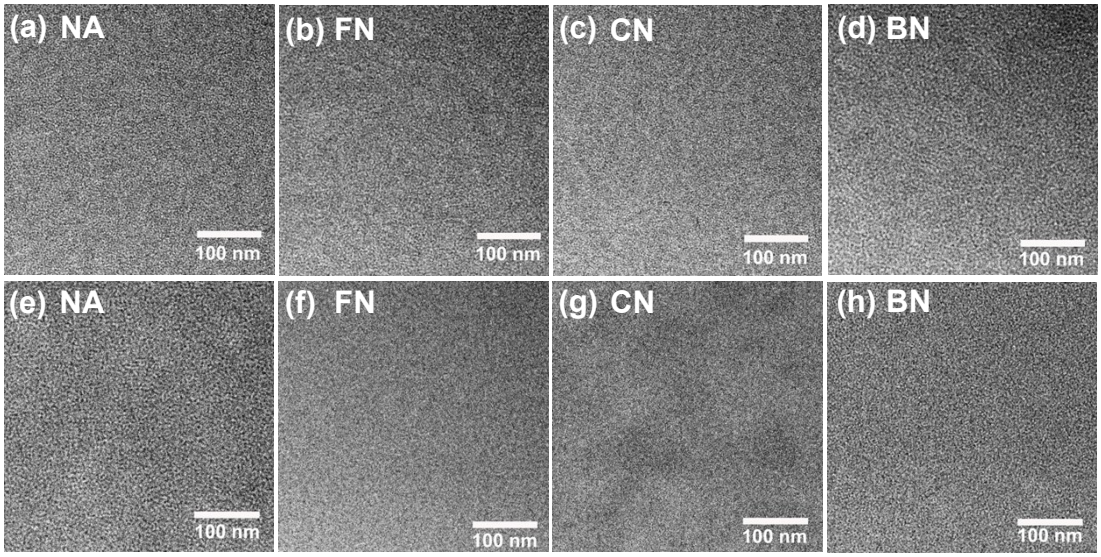

Figure S13. TEM images of PM6 pristine film of (a) NA, (b) FN, (c) CN, (d) BN and TEM images of Y6 pristine film of (e) NA, (f) FN, (g) CN and (h) BN;

10. *J-V* curves with varied incident light intensity

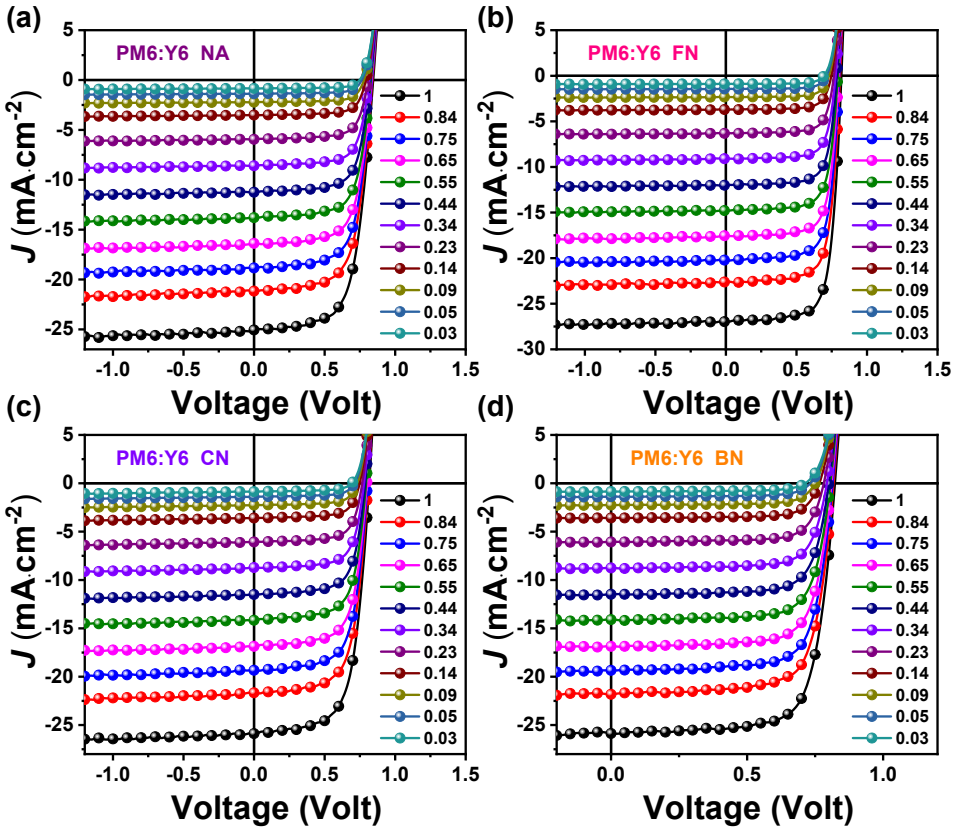

Figure S14. *J-V* curves with various incident light intensities of (a) NA, (b) FN, (c) CN and (d) BN devices.

11. Transient photovoltage (TPV) and transient photocurrent (TPC)

For TPV, the measurement was conducted under 1 sun conditions by illuminating the device with a white light-emitting diode, and the champion device is set to the open-circuit condition. For TPC, the champion device is set to the short-circuit condition in dark. The output signal was collected by keysight oscilloscope.

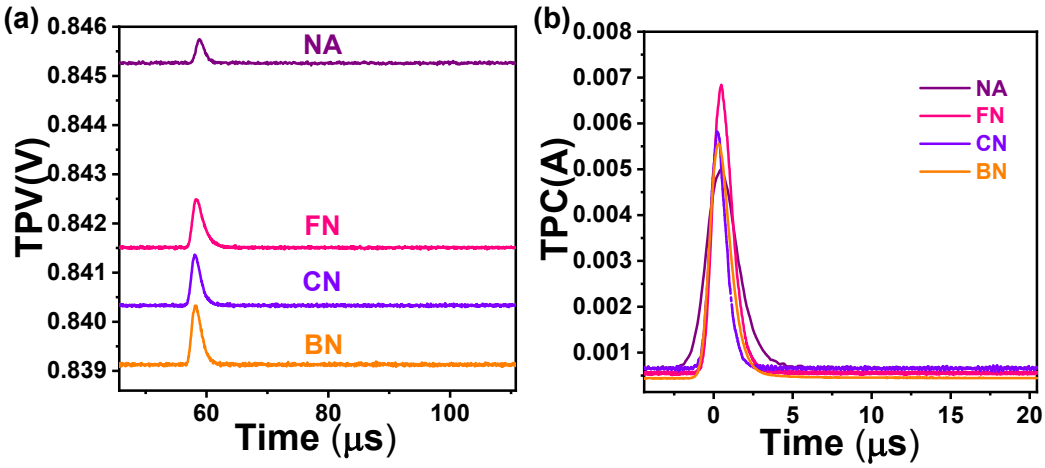

Figure S15. (a) TPV and (b) TPC of the PM6: Y6 devices processed with NA, FN, CN, and BN.

12. SCLC Measurements

Fitting the hole/electron-only diode dark current to the space charge limited current (SCLC) model can obtain the hole and electron mobility of the photosensitive active layer.The electron-only device structure was ITO/ZnO/ PFNBr/ BHJ/ PFNBr /Ag, and the hole-only device structure was ITO/PEDOT:PSS/BHJ/MoO_3/Ag. Using the following equation to estimate the electric-field dependent SCLC mobility:

$$J(V) = \frac{9}{8}\varepsilon_0\varepsilon_r\mu_0 exp\left(0.89\beta\sqrt{\frac{V - V_{bi}}{L}}\right)\frac{(V - V_{bi})^2}{L^3} \quad (3)$$

For the hole-only device structure, V_{bi} = 0 V (flat band pattern formed by PEDOT:PSS-MoO_3); For the electron-only device structure, V_{bi} = 0.5 V was used following the protocol reported.

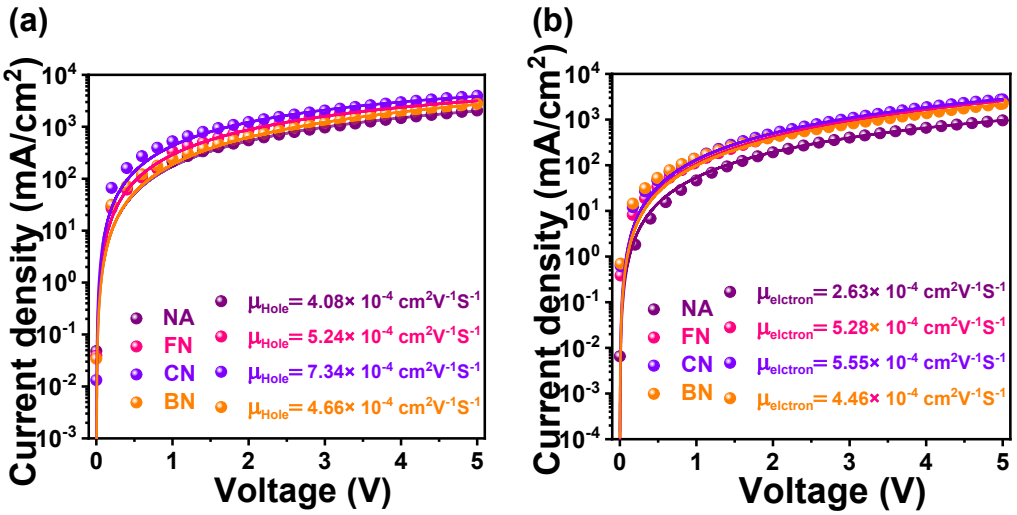

Figure S16. Dark J–V curves of the NA, FN, CN, BN OSCs: (a) electron-only diodes and (b) hole-only diodes; The solid lines are fit to the experimental data according to the equation **(3)**.

Table S7. Summary of carrier mobilities

Active layer	**μ_h [×10^{-4} cm^2 V^{-1} s^{-1}]**	**μ_e [×10^{-4} cm^2 V^{-1} s^{-1}]**	**μ_h /μ_e**
Non-additive	4.08±0.11	2.63±0.31	1.55
FN	5.24±0.14	5.28±0.19	0.99
CN	7.34±0.43	5.55±0.31	1.38
BN	4.66±0.30	4.46±0.11	1.04

13. Device statistics

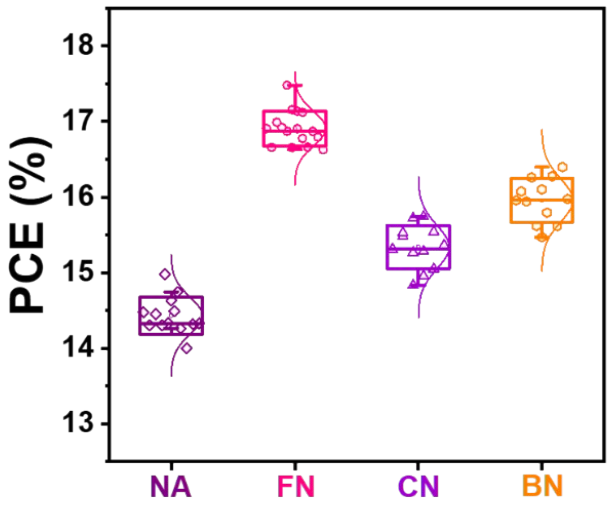

Figure S17. The PCE statistics of PM6:Y6 with NA, FN, CN and BN.

14. reference

1. M.-C. Michalski, J. Hardy and B. J. V. Saramago, *J. Colloid Interface Sci.*, 1998, **208**, 319-328.
2. D. K. Owens and R. C. Wendt, *J. Appl. Polym. Sci.*, 1969, **13**, 1741-1747.
3. Z. Cao, J. Chen, S. Liu, M. Qin, T. Jia, J. Zhao, Q. Li, L. Ying, Y.-P. Cai, X. Lu, F. Huang and Y. Cao, *Chem. Mater.*, 2019, **31**, 8533-8542.
4. S. Pang, R. Zhang, C. Duan, S. Zhang, X. Gu, X. Liu, F. Huang and Y. Cao, *Adv. Energy Mater.*, 2019, **9**, 1901740.
5. Y. Firdaus, L. P. Maffei, F. Cruciani, M. A. Müller, S. Liu, S. Lopatin, N. Wehbe, G. O. N. Ndjawa, A. Amassian, F. Laquai and P. M. Beaujuge, *Adv. Energy Mater.*, 2017, **7**, 1700834.
6. J. Wu, G. Li, J. Fang, X. Guo, L. Zhu, B. Guo, Y. Wang, G. Zhang, L. Arunagiri, F. Liu, H. Yan, M. Zhang and Y. Li, *Nat. Commun.*, 2020, **11**, 4612.